

# Quantum melting a Wigner crystal into Hall liquids

Aidan P. Reddy\* and Liang Fu

Department of Physics, Massachusetts Institute of Technology, Cambridge, Massachusetts 02139, USA

(Dated: August 29, 2025)

Recent experiments have shown that, counterintuitively, applying a magnetic field to a Wigner crystal can induce quantum Hall effects. In this work, using variational Monte Carlo, we show that magnetic fields can melt zero-field Wigner crystals into integer quantum Hall liquids. This melting originates from quantum oscillations in the liquid's ground state energy, which develops downward cusps at integer filling factors due to incompressibility. Our calculations establish a range of densities in which this quantum melting transition occurs.

*Introduction*— When Coulomb interactions overwhelm kinetic energy, an electron gas inevitably crystallizes [1, 2]. According to quantum Monte Carlo calculations [3–8], this zero-temperature freezing transition occurs at an interaction strength of  $r_s \approx 37$  in two dimensions. Evidence for Wigner crystals has been observed in several material systems at both strong [9–14] and zero [15–21] magnetic fields.

How does an out-of-plane magnetic field influence electron crystallization? Applying a magnetic field  $B$  to a Wigner crystal monotonically reduces its electrons' quantum zero-point motion [22, 23]. In contrast, applying a magnetic field to a Fermi liquid induces quantum Hall states accompanied by quantum oscillations that are periodic in  $1/B$ . Because electron liquids and crystals respond differently to magnetic fields, the liquid-crystal phase boundary should depend strongly on field strength, calling for theoretical and experimental study.

In this work, we apply variational Monte Carlo (VMC) to determine the quantum phase diagram of the fully-spin-polarized two-dimensional electron gas (2DEG) at integer Landau level fillings  $\nu$ . We use a unified Slater-Jastrow wavefunction to describe both electron crystal and Hall liquid phases. At  $\nu = 1$  and 2, we find phase transitions between integer quantum Hall states and electron crystals at critical interaction strengths of  $r_s \approx 47$  and  $\approx 39$ , significantly larger than the value  $r_s \approx 33$  for the transition between the fully-spin-polarized Fermi liquid and Wigner crystal at  $B = 0$  [6, 8]. Thus, our study reveals that quantum Hall states penetrate into the Wigner crystal region of the  $n - B$  plane, as shown in Fig. 1(b). Our theory explains the puzzling observation in ZnO-based 2DEGs that applying a magnetic field to a Wigner crystal can induce quantum Hall effects [19].

Additionally, we show that, at long wavelengths, the static structure factor is directly tied to the magneto-plasmon dispersion relation and shows universal behavior across the Hall liquid and Wigner crystal phases.

Before presenting detailed calculations, in Fig. 1(a) we sketch the ground state energy  $E$  of liquid and crystal phases as a function of  $B$  at a density slightly below the onset of Wigner crystallization at  $B = 0$ . The liquid's

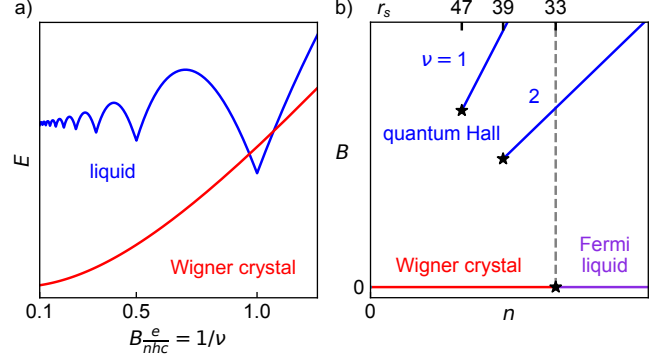


FIG. 1. **Quantum melting a Wigner crystal into Hall liquids.** (a) Schematic energies of liquid and crystal phases versus magnetic field  $B$ , at a density slightly below the zero-field crystallization point. (b)  $T = 0$  phase diagram of the fully-spin-polarized 2DEG in the  $n - B$  plane. The stars mark phase boundaries estimated from our variational Monte Carlo at  $\nu = 1, 2$  and  $B = 0$ . The dashed line marks the zero-field crystallization density.

energy oscillates as a function of  $\nu \propto 1/B$  with downward cusps at integer  $\nu$  due to the formation of incompressible quantum Hall states. In contrast, the crystal's energy is expected to increase smoothly as a function of  $B$  due to an increase in electron's zero-point energy. As a result of the different behaviors in  $E(B)$ , the liquid's energy dips below the crystal's in a range of magnetic fields near integer  $\nu$ , causing a transition from crystal to liquid states. This implies a density window in which a Wigner crystal present at  $B = 0$  melts into quantum Hall liquids, as illustrated in Fig. 1(b).

*Model*— We consider a system of spinless electrons in two dimensions interacting through a Coulomb potential in a homogeneous, out-of-plane magnetic field. This system has the Hamiltonian

$$H = \sum_i \frac{\pi_i^2}{2m} + \sum_{i < j} \frac{e^2}{|\mathbf{r}_i - \mathbf{r}_j|} \quad (1)$$

where  $\pi_i = \mathbf{p}_i + \frac{e}{c} \mathbf{A}(\mathbf{r}_i)$  and  $\nabla \times \mathbf{A} = -B\hat{z}$ . Full spin polarization is likely to occur at densities and magnetic field strengths of interest.

Our system involves three independent energy scales: the kinetic energy  $\hbar^2 n/m$  (where  $n$  is the electron den-

\* areddy@mit.edu

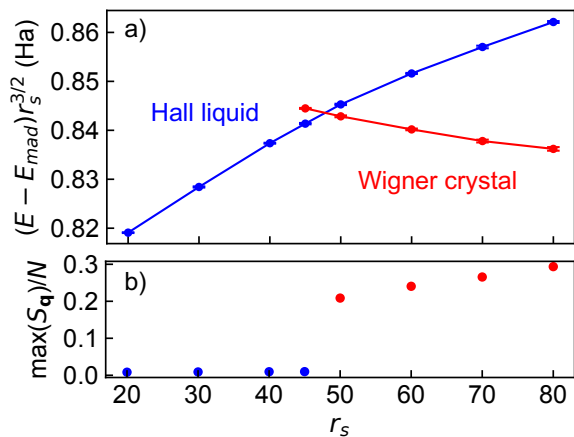


FIG. 2. **Quantum phase diagram at  $\nu = 1$ .** (a) Variational energies per particle obtained from the quantum Hall liquid and Wigner crystal ansätze as a function of  $r_s$ , indicating a phase transition near  $r_s \approx 47$ . Error bars indicate one standard error from binning analysis and  $E_{\text{mad}} = -1.106103 \text{ Ha}/r_s$  is the Madelung energy. (b) Maximum of the static structure factor of the optimized ground state, showing a sharp increase at the transition.  $N = 144$ .

sity), the interaction energy  $e^2\sqrt{n}$ , and the cyclotron energy  $\hbar\omega_c$  with cyclotron frequency  $\omega_c = \frac{eB}{mc}$ . The ratio of the interaction and kinetic energies defines the dimensionless interaction strength parameter:  $r_s = 1/\sqrt{\pi a_B^2 n}$  where  $a_B = \frac{\hbar^2}{e^2 m}$  is the Bohr radius. Similarly, the ratio of interaction and cyclotron energies defines the Landau level mixing parameter

$$\kappa = \frac{e^2}{\ell\hbar\omega_c} = r_s \sqrt{\frac{\nu}{2}} \quad (2)$$

where  $\ell = \sqrt{\frac{\nu}{2\pi n}} = \sqrt{\frac{\hbar c}{eB}}$  is the magnetic length and  $\nu = 2\pi\ell^2 n$  is the Landau level filling factor. The two dimensionless parameters  $r_s$  and  $\nu$  determine our system's phase diagram.

*Hartree-Fock and Lindemann analysis*– Before presenting our VMC analysis, we summarize two simpler approaches to the problem at hand: Hartree-Fock theory and the Lindemann melting criterion. Hartree-Fock theory predicts a liquid-to-crystal transition at  $r_s \approx 2.7$  when  $B = 0$  [24] and  $r_s \approx 9.6$  when  $\nu = 1$  [18, 25]. However, both of these values are much smaller than the estimates of  $r_s \approx 33$  from diffusion Monte Carlo calculations at  $B = 0$  [8] and  $r_s \approx 47$  from our VMC calculations  $\nu = 1$ . The Lindemann melting criterion asserts that the Wigner crystal melts when  $\gamma = \sqrt{\langle \mathbf{u}^2 \rangle}/a_{\text{WC}}$  exceeds a critical value  $\gamma^*$ , where  $a_{\text{WC}}$  is the lattice constant. This heuristic fails to capture magnetic-field-induced melting because, within the harmonic approximation,  $\sqrt{\langle \mathbf{u}^2 \rangle}$  monotonically decreases as a function of  $B$  [23, 25]. These theories' inadequacies call for a more accurate approach.

*Variational Monte Carlo methods*– To model both liq-

uid and crystal states, we use a unified Slater-Jastrow wavefunction with a homogeneous two-body Jastrow factor:

$$\Psi(R) = \det[\psi_i(\mathbf{r}_j)] \exp\left(\sum_{i<j} u(\mathbf{r}_i - \mathbf{r}_j)\right) \quad (3)$$

where  $R = (\mathbf{r}_1, \dots, \mathbf{r}_N)$  and  $N$  is the number of electrons. We impose the magnetic quasi-periodic boundary condition  $t_i(\mathbf{L})\Psi(R) = \Psi(R)$  where  $\mathbf{L}$  is a supercell lattice vector and  $t_i$  is a magnetic translation operator for particle  $i$  [26–28]. To satisfy this boundary condition, we expand each single-particle orbital  $|\psi_{\mathbf{k}n}\rangle$  in the Slater determinant as a linear combination of Landau level orbitals  $|\phi_{\mathbf{k}n}\rangle$ , which comprise an orthogonal basis for the boundary condition. Concretely, we write

$$|\psi_{\mathbf{k}m}\rangle = \sum_{n=0}^{n_{\text{max}}} U_{mn}^{\mathbf{k}} |\phi_{\mathbf{k}n}\rangle \quad (4)$$

where  $U_{mn}^{\mathbf{k}}$  is a unitary orbital rotation matrix [25]. Here  $n$  is a Landau level index and  $\mathbf{k}$  is a wavevector in the magnetic Brillouin zone. Each row of the Slater matrix  $\psi_i(\mathbf{r}_j)$  corresponds to one of the orbitals  $|\psi_{\mathbf{k}m}\rangle$ , for  $0 \leq m < \nu$  and every  $\mathbf{k}$ . This construction yields the most general Slater determinant consistent with the magnetic unit cell, chosen to match the Wigner crystal, up to the Landau level cutoff  $n_{\text{max}}$ .

The variational parameters of our wavefunction are contained in  $u(\mathbf{r})$  and the orbital rotation matrix  $U_{mn}^{\mathbf{k}}$ . Using the stochastic reconfiguration algorithm [29, 30], we optimize these parameters to minimize the energy expectation value of  $\Psi(R)$ . For each  $r_s$ , we initialize and constrain the parameters in two ways. For the liquid phase, we optimize only  $u(\mathbf{r})$  and set  $U_{mn}^{\mathbf{k}} = \delta_{mn}$  so that the determinant is the non-interacting ground state. For the Wigner crystal phase, we generate crystal “seed” orbitals by optimizing a randomly initialized determinant with a Jastrow factor at large  $r_s$ . For other values of  $r_s$ , we initialize the orbitals to this seed and then optimize them together with the Jastrow factor.

*Variational Monte Carlo phase diagram*– In Fig. 2(a), we show variational energies obtained from these two ansatzes at  $\nu = 1$  and several values of  $r_s$ . When  $r_s \geq 50$ , the crystal has lower energy, while for  $r_s \leq 45$ , the liquid is favored. A linear interpolation of the liquid and crystal energies between  $r_s = 45$  and  $50$  locates the melting transition at  $r_s \approx 47$ . We show analogous data at  $\nu = 2$  that indicate a phase transition near  $r_s \approx 39$  in the Supplemental Material [25].

Fig. 2(b) shows that the optimized ground state for  $r_s \gtrsim 50$  has Bragg peaks, indicating crystallization. Our wavefunction assumes magnetic translation symmetry with respect to the Wigner crystal lattice and is therefore incapable of describing microemulsion or other intermediate phases in which translation symmetry is broken at a longer length scale [31–33]. Bearing this caveat in mind,

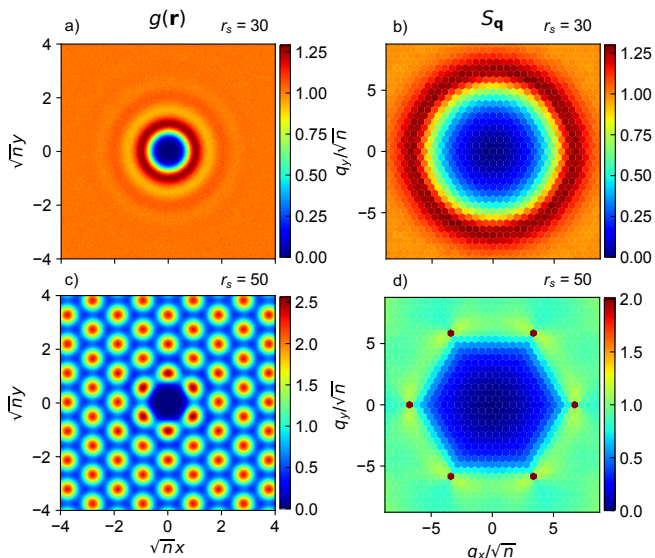


FIG. 3. **Density correlations at  $\nu = 1$ .** Pair correlation function (left) and static structure factor (right) of the optimized wavefunctions in the liquid (a,b) and crystal (c,d) phases. The color scale in (d) saturates and  $S_q \approx 30$  at the first shell of Bragg peaks (dark red points).  $N = 144$ .

the cusp in ground state energy and sharp discontinuity in the Bragg peak height at the phase boundary are consistent with a first-order melting transition.

The most recent diffusion Monte Carlo calculations available estimate the Fermi-liquid-to-Wigner-crystal transition in the fully-spin-polarized 2DEG at  $B = 0$  to occur at  $r_s \approx 33$  [8] (lower than  $r_s \approx 37$  in the presence of spin [7, 8]). To obtain a fairer comparison with our VMC results at  $B \neq 0$ , we perform a VMC calculation at  $B = 0$  and find  $r_s \approx 33$  [25], in agreement with Ref. [8]. This is significantly lower than the values  $r_s \approx 47$  and 39 we find at  $\nu = 1$  and 2. Therefore, there exists density window where a Wigner crystal forms at  $B = 0$  but melts into quantum Hall liquids at small integer fillings.

*Density correlations and collective excitations*—Having established our system’s phase diagram, we now examine the properties of its liquid and crystal phases. In Fig. 3(a,b) we show density correlation functions of the optimized wavefunction at  $r_s = 30$ . The static structure factor,

$$S_q = \frac{1}{N} \sum_{i,j} \langle \Psi | e^{i\mathbf{q} \cdot (\mathbf{r}_i - \mathbf{r}_j)} | \Psi \rangle, \quad (5)$$

peaks smoothly around the reciprocal lattice vector  $Q_{\text{WC}} = \sqrt{\frac{8\pi^2}{3}}n$  of a Wigner crystal. Similarly, the pair correlation function,

$$g(\mathbf{r}) = \frac{A}{N^2} \sum_{i \neq j} \langle \Psi | \delta^2(\mathbf{r} - \mathbf{r}_i + \mathbf{r}_j) | \Psi \rangle, \quad (6)$$

peaks smoothly around the lattice constant  $a_{\text{WC}} = \sqrt{\frac{2}{\sqrt{3}n}}$  of a Wigner crystal. These features are typical

of a strongly correlated liquid. In contrast, the density correlation functions at  $r_s = 60$  shown in Fig. 3(c,d) reveal crystallization. The real-space pair correlation function exhibits periodic modulation throughout the system. This long-range order appears as Bragg peaks in the static structure factor at the reciprocal lattice vector  $Q_{\text{WC}}\hat{x}$  and its  $\pi/3$  rotations.

We now relate our system’s long-wavelength density-density correlations to its collective excitations. Classically, a two-dimensional electron liquid in an out-of-plane magnetic field interacting through a Coulomb potential  $v(q) = 2\pi e^2/q$  has a longitudinal collective excitation mode, the magnetoplasmon, with a dispersion relation

$$\omega_p(q) = \sqrt{\omega_c^2 + \frac{2\pi e^2 n}{m} q}. \quad (7)$$

Quantum mechanically, the magnetoexciton of the integer quantum Hall state and longitudinal phonon of the Wigner crystal follow this dispersion relation at small  $q$ , as can be shown rigorously in the limits of small and large  $r_s$  [34–36]. In the limit  $B \rightarrow 0$ , the plasmon dispersion of a 2D Coulomb gas,  $\omega_p(q) = \sqrt{\frac{2\pi e^2 n}{m} q}$ , is recovered.

Let us assume that this collective mode exists in the quantum system and exhausts the  $f$ -sum rule at generic  $r_s$ . Under this assumption, the static structure factor obeys

$$S_q = \frac{\hbar q^2}{2m\omega_p(q)} = \frac{\ell^2}{2} q^2 - \frac{\kappa\nu\ell^3}{4} q^3 + \mathcal{O}(q^4) \quad (8)$$

at small  $q$ . The leading  $\mathcal{O}(q^2)$  term is an exact property of the quantum system guaranteed by Kohn’s theorem [37] – that is, the optical spectral weight is completely exhausted by the cyclotron mode due to the decoupling between electrons’ center-of-mass and relative degrees of freedom. In the quantum Hall phase, the property  $\lim_{q \rightarrow 0} S_q/q^2 \geq \frac{\ell^2}{2}$  is also required by the system’s topologically quantized Hall conductance  $\sigma_H = \nu e^2/h$  [38, 39]. The subleading  $\mathcal{O}(q^3)$  term, which is non-analytic as a function of  $q$ , is a consequence of the Coulomb interaction in gapped two-dimensional systems.

In Fig. 4, we test this assumption by comparing  $\hbar\omega_p(q)$  with the single-mode approximation dispersion,  $\Delta(q) \equiv \frac{\hbar^2 q^2}{2mS_q}$ , across a wide range of interaction strengths [40].  $\hbar\omega_p(q)$  and  $\Delta(q)$  converge as  $q \rightarrow 0$  in both the liquid and Wigner crystal phases. This supports the existence of a magnetoplasmon mode that exhausts the  $f$ -sum rule in the limit  $q \rightarrow 0$  for all  $r_s$ . It also shows that our wavefunctions respect Kohn’s theorem. We emphasize that this behavior is not enforced by construction but rather obtained through optimization, signaling that our wavefunctions are accurate. Additionally, when  $r_s$  is large,  $\Delta(q)$  shows a roton minimum near  $Q_{\text{WC}}$ . This rather generic feature of strongly interacting quantum liquids is a direct consequence of the peak in  $S_q$  and reflects strong short-range correlations [40, 41].

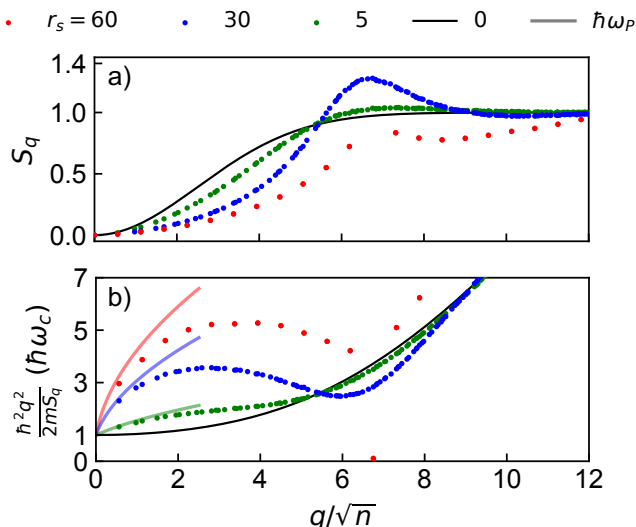


FIG. 4. **Static structure factor and magnetoplasmons.** (a) Static structure factor  $S_q$  of the variational ground state at  $\nu = 1$ . (b) Dispersion of longitudinal collective modes from the single-mode approximation, which converges with the classical magnetoplasmon dispersion (semi-transparent lines) at small  $q$ . The data are rotation-averaged in the liquid phase and taken along the  $x$ -axis in the crystal phase.  $N = 144$ .

*Discussion*— We have shown that a magnetic field can melt a Wigner crystal into quantum Hall liquids at small integer Landau level fillings. Using the variational Monte Carlo method, we have computed the quantum phase diagram of the fully spin-polarized 2DEG at  $\nu = 1$  and 2. We find phase transitions between integer quantum Hall and Wigner crystal states at  $r_s \approx 47$  and 39 respectively. These interaction strengths are larger than the  $B = 0$  transition points,  $r_s \approx 37$  with spin and  $r_s \approx 33$  without spin [7, 8]. This establishes a density window in which a Wigner crystal present at  $B = 0$  melts into a quantum Hall state under a magnetic field. Experimentally, this implies that at fixed density the system is strongly insulating at zero field but exhibits a quantized Hall effect with  $R_{xx} = 0$  at small integer fillings, as observed in Ref. [19]. Finally, we have shown that magnetoplasmon collective excitations control the system’s long-wavelength density correlations, which exhibit unified behavior across both liquid and crystal phases.

To our knowledge, our work is the first beyond-mean-field study of the spinless 2DEG phase diagram at integer  $\nu$ . While we have focused on integer  $\nu$ , simi-

lar magnetic-field-induced transitions between liquid and crystal phases also occur at fractional Landau Level filling. For example, at small  $\nu < 1$ , electron crystal phases are interrupted by fractional quantum Hall liquids at special fractions such as  $\frac{1}{3}$  or  $\frac{1}{5}$ , as has been observed in multiple material systems [11, 14, 42–51] and studied theoretically, including by QMC methods [52–59].

When these liquid-crystal oscillations occur in higher Landau levels, they lead to “reentrant integer quantum Hall effects” [60–65]. In some moiré systems at  $B = 0$ , integer quantum anomalous Hall states are observed over a broad range of densities, except certain fractional band fillings where fractional quantum anomalous Hall states form [66, 67]. These phenomena likely also originate from downward cusps in the liquid’s energy due to incompressibility that bring it below the energy of competing crystal phases (see Fig. 1(b)).

Our work invites further research in related directions. One natural extension is to explore the influence of a moiré potential, which can give rise to generalized Wigner crystals [68–73]. Another compelling direction is to investigate interplay between magnetic fields and Wigner crystallization in few-layer graphene systems, which feature unconventional band dispersions and large Berry curvature [14]. Crystallization at  $B = 0$  in flat bands with Berry curvature is also an intriguing possibility to address numerically beyond the Hartree-Fock approximation [74–83]. More broadly, microscopic mechanisms for coexistence between crystallization and topology—whether at zero or finite magnetic field—remain to be explored [84, 85]. Finally, it may be possible to combine aspects of our wavefunction ansatz with neural networks to study competing liquid and crystal phases in quantum Hall systems and Chern bands [86–89].

*Acknowledgments*— We thank Max Geier, Yaar Vituri, Bryan Clark, Shiwei Zhang, Agnes Valenti, David Dai, Patrick Ledwith, and Khachatur Nazaryan for helpful discussions. AR is particularly grateful to Ahmed Abouelkomsan for numerous helpful discussions and encouragement. The authors acknowledge the MIT SuperCloud and Lincoln Laboratory Supercomputing Center for providing computing resources that have contributed to the research results reported in this paper. This work was supported by the U.S. Army DEVCOM ARL Army Research Office through the MIT Institute for Soldier Nanotechnologies under Cooperative Agreement number W911NF-23-2-0121. LF was supported by a Simons Investigator Award from the Simons Foundation.

[1] E. Wigner, On the interaction of electrons in metals, *Physical Review* **46**, 1002 (1934).  
 [2] Y. P. Monarkha and V. Syvokon, A two-dimensional wigner crystal, *Low Temperature Physics* **38**, 1067 (2012).  
 [3] D. Ceperley, Ground state of the fermion one-component

plasma: A monte carlo study in two and three dimensions, *Physical Review B* **18**, 3126 (1978).  
 [4] B. Tanatar and D. M. Ceperley, Ground state of the two-dimensional electron gas, *Physical Review B* **39**, 5005 (1989).  
 [5] C. Attacalite, S. Moroni, P. Gori-Giorgi, and G. B.

- Bachelet, Correlation energy and spin polarization in the 2d electron gas, *Physical review letters* **88**, 256601 (2002).
- [6] N. Drummond and R. Needs, Quantum monte carlo study of the ground state of the two-dimensional fermi fluid, *Physical Review B—Condensed Matter and Materials Physics* **79**, 085414 (2009).
- [7] C. Smith, Y. Chen, R. Levy, Y. Yang, M. A. Morales, and S. Zhang, Unified variational approach description of ground-state phases of the two-dimensional electron gas, *Physical Review Letters* **133**, 266504 (2024).
- [8] S. Azadi, N. Drummond, and S. M. Vinko, Quantum monte carlo study of the phase diagram of the two-dimensional uniform electron liquid, *Physical Review B* **110**, 245145 (2024).
- [9] E. Andrei, G. Deville, D. Glatli, F. Williams, E. Paris, and B. Etienne, Observation of a magnetically induced wigner solid, *Physical review letters* **60**, 2765 (1988).
- [10] H. Stormer and R. Willett, Comment on “observation of a magnetically induced wigner solid”, *Physical Review Letters* **62**, 972 (1989).
- [11] V. Goldman, M. Santos, M. Shayegan, and J. Cunningham, Evidence for two-dimensional quantum wigner crystal, *Physical review letters* **65**, 2189 (1990).
- [12] F. Williams, P. Wright, R. Clark, E. Andrei, G. Deville, D. Glatli, O. Probst, B. Etienne, C. Dorin, C. Foxon, *et al.*, Conduction threshold and pinning frequency of magnetically induced wigner solid, *Physical review letters* **66**, 3285 (1991).
- [13] M. Paalanen, R. Willett, R. Ruel, P. Littlewood, K. West, and L. Pfeiffer, Electrical conductivity and wigner crystallization, *Physical Review B* **45**, 13784 (1992).
- [14] Y.-C. Tsui, M. He, Y. Hu, E. Lake, T. Wang, K. Watanabe, T. Taniguchi, M. P. Zaletel, and A. Yazdani, Direct observation of a magnetic-field-induced wigner crystal, *Nature* **628**, 287 (2024).
- [15] J. Yoon, C. Li, D. Shahar, D. Tsui, and M. Shayegan, Wigner crystallization and metal-insulator transition of two-dimensional holes in gaas at  $b = 0$ , *Physical review letters* **82**, 1744 (1999).
- [16] R. L. Qiu, X. Gao, L. Pfeiffer, and K. West, Connecting the reentrant insulating phase and the zero-field metal-insulator transition in a 2d hole system, *Physical review letters* **108**, 106404 (2012).
- [17] M. S. Hossain, M. Ma, K. V. Rosales, Y. Chung, L. Pfeiffer, K. West, K. Baldwin, and M. Shayegan, Observation of spontaneous ferromagnetism in a two-dimensional electron system, *Proceedings of the National Academy of Sciences* **117**, 32244 (2020).
- [18] T. Smoleński, P. E. Dolgirev, C. Kuhlenkamp, A. Popert, Y. Shimazaki, P. Back, X. Lu, M. Kroner, K. Watanabe, T. Taniguchi, *et al.*, Signatures of wigner crystal of electrons in a monolayer semiconductor, *Nature* **595**, 53 (2021).
- [19] J. Falson, I. Sodemann, B. Skinner, D. Tabrea, Y. Kozuka, A. Tsukazaki, M. Kawasaki, K. von Klitzing, and J. H. Smet, Competing correlated states around the zero-field wigner crystallization transition of electrons in two dimensions, *Nature materials* **21**, 311 (2022).
- [20] S. Munyan, S. Ahadi, B. Guo, A. Rashidi, and S. Stemmer, Evidence of zero-field wigner solids in ultrathin films of cadmium arsenide, *Physical Review X* **14**, 041037 (2024).
- [21] Z. Xiang, H. Li, J. Xiao, M. H. Naik, Z. Ge, Z. He, S. Chen, J. Nie, S. Li, Y. Jiang, *et al.*, Imaging quantum melting in a disordered 2d wigner solid, *Science* **388**, 736 (2025).
- [22] Y. E. Lozovik and V. Yudson, Crystallization of a two-dimensional electron gas in a magnetic field, *ZhETF Pisma Redaktsiiu* **22**, 26 (1975).
- [23] F. Ulinich and N. Usov, Phase diagram of a two-dimensional wigner crystal in a magnetic field, *Sov. Phys. JETP* **49**, 147 (1979).
- [24] B. Bernu, F. Delyon, M. Duneau, and M. Holzmann, Metal-insulator transition in the hartree-fock phase diagram of the fully polarized homogeneous electron gas in two dimensions, *Physical Review B—Condensed Matter and Materials Physics* **78**, 245110 (2008).
- [25] See the Supplemental Material for additional results, methodology, and a discussion of earlier calculations in the literature at  $B = 0$ .
- [26] F. Haldane, Many-particle translational symmetries of two-dimensional electrons at rational landau-level filling, *Physical review letters* **55**, 2095 (1985).
- [27] E. Brown, Bloch electrons in a uniform magnetic field, *Physical Review* **133**, A1038 (1964).
- [28] J. Zak, Magnetic translation group, *Physical Review* **134**, A1602 (1964).
- [29] S. Sorella, Generalized lanczos algorithm for variational quantum monte carlo, *Physical Review B* **64**, 024512 (2001).
- [30] F. Becca and S. Sorella, *Quantum Monte Carlo approaches for correlated systems* (Cambridge University Press, 2017).
- [31] B. Spivak, Phase separation in the two-dimensional electron liquid in mosfet’s, *Physical Review B* **67**, 125205 (2003).
- [32] B. Spivak and S. A. Kivelson, Phases intermediate between a two-dimensional electron liquid and wigner crystal, *Physical Review B—Condensed Matter and Materials Physics* **70**, 155114 (2004).
- [33] J. Sung, J. Wang, I. Esterlis, P. A. Volkov, G. Scuri, Y. Zhou, E. Brutschea, T. Taniguchi, K. Watanabe, Y. Yang, *et al.*, An electronic microemulsion phase emerging from a quantum crystal-to-liquid transition, *Nature Physics* **21**, 437 (2025).
- [34] C. Kallin and B. Halperin, Excitations from a filled landau level in the two-dimensional electron gas, *Physical Review B* **30**, 5655 (1984).
- [35] A. MacDonald, Hartree-fock approximation for response functions and collective excitations in a two-dimensional electron gas with filled landau levels, *Journal of Physics C: Solid State Physics* **18**, 1003 (1985).
- [36] L. Bonsall and A. Maradudin, Some static and dynamical properties of a two-dimensional wigner crystal, *Physical Review B* **15**, 1959 (1977).
- [37] W. Kohn, Cyclotron resonance and de haas-van alphen oscillations of an interacting electron gas, *Physical Review* **123**, 1242 (1961).
- [38] Y. Onishi and L. Fu, Topological bound on the structure factor, *Physical Review Letters* **133**, 206602 (2024).
- [39] Y. Onishi and L. Fu, Quantum weight: A fundamental property of quantum many-body systems, *Physical Review Research* **7**, 023158 (2025).
- [40] R. P. Feynman, Atomic theory of the two-fluid model of liquid helium, *Physical Review* **94**, 262 (1954).
- [41] S. Girvin, A. MacDonald, and P. Platzman, Magneto-roton theory of collective excitations in the fractional

- quantum hall effect, *Physical Review B* **33**, 2481 (1986).
- [42] H. Jiang, R. Willett, H. Stormer, D. Tsui, L. Pfeiffer, and K. West, Quantum liquid versus electron solid around  $\nu=1/5$  Landau-level filling, *Physical review letters* **65**, 633 (1990).
- [43] Y. P. Li, T. Sajoto, L. Engel, D. Tsui, and M. Shayegan, Low-frequency noise in the reentrant insulating phase around the  $1/5$  fractional quantum hall liquid, *Physical review letters* **67**, 1630 (1991).
- [44] H. Jiang, H. Stormer, D. Tsui, L. Pfeiffer, and K. West, Magnetotransport studies of the insulating phase around  $\nu=1/5$  Landau-level filling, *Physical Review B* **44**, 8107 (1991).
- [45] M. Santos, Y. Suen, M. Shayegan, Y. Li, L. Engel, and D. Tsui, Observation of a reentrant insulating phase near the  $1/3$  fractional quantum hall liquid in a two-dimensional hole system, *Physical review letters* **68**, 1188 (1992).
- [46] D. Maryenko, A. McCollam, J. Falson, Y. Kozuka, J. Bruin, U. Zeitler, and M. Kawasaki, Composite fermion liquid to wigner solid transition in the lowest Landau level of zinc oxide, *Nature communications* **9**, 4356 (2018).
- [47] S. Chen, R. Ribeiro-Palau, K. Yang, K. Watanabe, T. Taniguchi, J. Hone, M. O. Goerbig, and C. R. Dean, Competing fractional quantum hall and electron solid phases in graphene, *Physical review letters* **122**, 026802 (2019).
- [48] M. K. Ma, K. Villegas Rosales, H. Deng, Y. Chung, L. Pfeiffer, K. West, K. Baldwin, R. Winkler, and M. Shayegan, Thermal and quantum melting phase diagrams for a magnetic-field-induced wigner solid, *Physical review letters* **125**, 036601 (2020).
- [49] K. Villegas Rosales, S. Singh, M. K. Ma, M. S. Hossain, Y. Chung, L. Pfeiffer, K. West, K. Baldwin, and M. Shayegan, Competition between fractional quantum hall liquid and wigner solid at small fillings: Role of layer thickness and Landau level mixing, *Physical Review Research* **3**, 013181 (2021).
- [50] Y.-j. Dong, X. Wang, J. Zheng, W. Qiao, R.-R. Du, L. N. Pfeiffer, K. W. West, and K. W. Baldwin, Nonlinear transport of wigner solid phase surrounding the two-flux composite fermion liquid, *Physical Review Research* **7**, L022011 (2025).
- [51] A. Haug, R. Kumar, T. Firon, M. Yutushui, K. Watanabe, T. Taniguchi, D. F. Mross, and Y. Ronen, Interaction-driven quantum phase transitions between topological and crystalline orders of electrons, *arXiv. org* (2025).
- [52] P. K. Lam and S. Girvin, Liquid-solid transition and the fractional quantum-hall effect, *Physical Review B* **30**, 473 (1984).
- [53] D. Levesque, J. Weis, and A. MacDonald, Crystallization of the incompressible quantum-fluid state of a two-dimensional electron gas in a strong magnetic field, *Physical Review B* **30**, 1056 (1984).
- [54] X. Zhu and S. G. Louie, Wigner crystallization in the fractional quantum hall regime: A variational quantum monte carlo study, *Physical review letters* **70**, 335 (1993).
- [55] G. Ortiz, D. Ceperley, and R. Martin, New stochastic method for systems with broken time-reversal symmetry: 2d fermions in a magnetic field, *Physical review letters* **71**, 2777 (1993).
- [56] R. Price, P. Platzman, and S. He, Fractional quantum hall liquid, wigner solid phase boundary at finite density and magnetic field, *Physical review letters* **70**, 339 (1993).
- [57] X. Zhu and S. G. Louie, Variational quantum monte carlo study of two-dimensional wigner crystals: Exchange, correlation, and magnetic-field effects, *Physical Review B* **52**, 5863 (1995).
- [58] A. C. Archer, K. Park, and J. K. Jain, Competing crystal phases in the lowest Landau level, *Physical review letters* **111**, 146804 (2013).
- [59] J. Zhao, Y. Zhang, and J. Jain, Crystallization in the fractional quantum hall regime induced by Landau-level mixing, *Physical review letters* **121**, 116802 (2018).
- [60] J. Eisenstein, K. Cooper, L. Pfeiffer, and K. West, Insulating and fractional quantum hall states in the first excited Landau level, *Physical Review Letters* **88**, 076801 (2002).
- [61] J. Xia, W. Pan, C. Vicente, E. Adams, N. Sullivan, H. Stormer, D. Tsui, L. Pfeiffer, K. Baldwin, and K. West, Electron correlation in the second Landau level: A competition between many nearly degenerate quantum phases, *Physical review letters* **93**, 176809 (2004).
- [62] A. Kumar, G. Csáthy, M. Manfra, L. Pfeiffer, and K. West, Nonconventional odd-denominator fractional quantum hall states in the second Landau level, *Physical review letters* **105**, 246808 (2010).
- [63] Y. Liu, C. Pappas, M. Shayegan, L. Pfeiffer, K. West, and K. Baldwin, Observation of reentrant integer quantum hall states in the lowest Landau level, *Physical Review Letters* **109**, 036801 (2012).
- [64] N. Deng, A. Kumar, M. J. Manfra, L. Pfeiffer, K. West, and G. A. Csathy, Collective nature of the reentrant integer quantum hall states in the second Landau level, *Physical review letters* **108**, 086803 (2012).
- [65] H. Zhou, H. Polshyn, T. Taniguchi, K. Watanabe, and A. Young, Solids of quantum hall skyrmions in graphene, *Nature Physics* **16**, 154 (2020).
- [66] Z. Lu, T. Han, Y. Yao, Z. Hadjri, J. Yang, J. Seo, L. Shi, S. Ye, K. Watanabe, T. Taniguchi, *et al.*, Extended quantum anomalous hall states in graphene/hBN moiré superlattices, *Nature* **637**, 1090 (2025).
- [67] F. Xu, Z. Sun, J. Li, C. Zheng, C. Xu, J. Gao, T. Jia, K. Watanabe, T. Taniguchi, B. Tong, *et al.*, Signatures of unconventional superconductivity near reentrant and fractional quantum anomalous hall insulators, *arxiv e-prints*, arXiv preprint arXiv:2504.06972 (2025).
- [68] G. Fedorovich, C. Kuhlenkamp, A. Imamoglu, and I. Amelio, First-order quantum hall to wigner crystal phase transition on a triangular lattice: An infinite density matrix renormalization group study, *Physical Review B* **111**, 235141 (2025).
- [69] Q. J. Zong, H. Wang, Q. Zhang, X. Cheng, Y. He, Q. Xu, A. Fischer, K. Watanabe, T. Taniguchi, D. A. Rhodes, *et al.*, Quantum melting of generalized electron crystal in twisted bilayer moiré, *Nature Communications* **16**, 4058 (2025).
- [70] G. Chen, Y.-H. Zhang, A. Sharpe, Z. Zhang, S. Wang, L. Jiang, B. Lyu, H. Li, K. Watanabe, T. Taniguchi, *et al.*, Magnetic field-stabilized wigner crystal states in a graphene moiré superlattice, *Nano Letters* **23**, 7023 (2023).
- [71] H. Li, S. Li, E. C. Regan, D. Wang, W. Zhao, S. Kahn, K. Yumigeta, M. Blei, T. Taniguchi, K. Watanabe, *et al.*, Imaging two-dimensional generalized wigner crystals, *Nature* **597**, 650 (2021).

- [72] E. C. Regan, D. Wang, C. Jin, M. I. Bakti Utama, B. Gao, X. Wei, S. Zhao, W. Zhao, Z. Zhang, K. Yumigeta, *et al.*, Mott and generalized wigner crystal states in wse<sub>2</sub>/ws<sub>2</sub> moiré superlattices, *Nature* **579**, 359 (2020).
- [73] Y. Xu, S. Liu, D. A. Rhodes, K. Watanabe, T. Taniguchi, J. Hone, V. Elser, K. F. Mak, and J. Shan, Correlated insulating states at fractional fillings of moiré superlattices, *Nature* **587**, 214 (2020).
- [74] P. Silvestrov and P. Recher, Wigner crystal phases in bilayer graphene, *Physical Review B* **95**, 075438 (2017).
- [75] S. Joy and B. Skinner, Wigner crystallization in bernal bilayer graphene, arXiv preprint arXiv:2310.07751 (2023).
- [76] T. Tan and T. Devakul, Parent berry curvature and the ideal anomalous hall crystal, *Physical Review X* **14**, 041040 (2024).
- [77] B. Zhou, H. Yang, and Y.-H. Zhang, Fractional quantum anomalous hall effect in rhombohedral multilayer graphene in the moiréless limit, *Physical Review Letters* **133**, 206504 (2024).
- [78] J. Dong, T. Wang, T. Wang, T. Soejima, M. P. Zaletel, A. Vishwanath, and D. E. Parker, Anomalous hall crystals in rhombohedral multilayer graphene. i. interaction-driven chern bands and fractional quantum hall states at zero magnetic field, *Physical Review Letters* **133**, 206503 (2024).
- [79] A. P. Reddy, F. Alsallom, Y. Zhang, T. Devakul, and L. Fu, Fractional quantum anomalous hall states in twisted bilayer mote 2 and wse 2, *Physical Review B* **108**, 085117 (2023).
- [80] A. P. Reddy and L. Fu, Toward a global phase diagram of the fractional quantum anomalous hall effect, *Physical Review B* **108**, 245159 (2023).
- [81] D. Sheng, A. P. Reddy, A. Abouelkomsan, E. J. Bergholtz, and L. Fu, Quantum anomalous hall crystal at fractional filling of moiré superlattices, *Physical Review Letters* **133**, 066601 (2024).
- [82] S. Joy, L. Levitov, and B. Skinner, Chiral wigner crystal phases induced by berry curvature, arXiv preprint arXiv:2507.22121 (2025).
- [83] K.-S. Kim, Magnetic interactions of wigner crystal in magnetic field and berry curvature: Multi-particle tunneling through complex trajectories, arXiv preprint arXiv:2508.13149 (2025).
- [84] S. Kivelson, C. Kallin, D. P. Arovas, and J. R. Schrieffer, Cooperative ring exchange theory of the fractional quantized hall effect, *Physical review letters* **56**, 873 (1986).
- [85] Z. Tešanović, F. Axel, and B. Halperin, “hall crystal” versus wigner crystal, *Physical Review B* **39**, 8525 (1989).
- [86] Y. Teng, D. D. Dai, and L. Fu, Solving the fractional quantum hall problem with self-attention neural network, *Physical Review B* **111**, 205117 (2025).
- [87] Y. Qian, T. Zhao, J. Zhang, T. Xiang, X. Li, and J. Chen, Describing landau level mixing in fractional quantum hall states with deep learning, *Physical Review Letters* **134**, 176503 (2025).
- [88] X. Li, Y. Chen, B. Li, H. Chen, F. Wu, J. Chen, and W. Ren, Deep learning sheds light on integer and fractional topological insulators, arXiv preprint arXiv:2503.11756 (2025).
- [89] D. Luo, T. Zaklana, and L. Fu, Solving fractional electron states in twisted mote<sub>2</sub> with deep neural network, arXiv preprint arXiv:2503.13585 (2025).